EARTHQUAKE ENGINEERING AND STRUCTURAL DYNAMICS
Earthquake Engng Struct. Dyn. 2012; **41**:1177–1197
Published online 24 November 2011 in Wiley Online Library (wileyonlinelibrary.com). DOI: 10.1002/eqe.1182

Rocking isolation of low-rise frame structures founded on isolated footings

F. Gelagoti, R. Kourkoulis, I. Anastasopoulos and G. Gazetas*,†

School of Civil Engineering, National Technical University of Athens, Athens, Greece

SUMMARY

This paper explores the effectiveness of a new approach to foundation seismic design. Instead of the present practice of over-design, the foundations are intentionally under-dimensioned so as to uplift and mobilize the strength of the supporting (stiff) soil, in the hope that they will thus act as a *rocking–isolation* mechanism, limiting the inertia transmitted to the superstructure, and guiding plastic 'hinging' into soil and the foundation–soil interface. An idealized simple but realistic one-bay two-story reinforced concrete moment resisting frame serves as an example to compare the two alternatives. The problem is analyzed employing the finite element method, taking account of material (*soil* and *superstructure*) and geometric (*uplifting* and *P–Δ effects*) nonlinearities. The response is first investigated through static pushover analysis. It is shown that the axial forces N acting on the footings and the moment to shear (M/Q) ratio fluctuate substantially during shaking, leading to significant changes in footing moment-rotation response. The seismic performance is explored through dynamic time history analyses, using a wide range of unscaled seismic records as excitation. It is shown that although the performance of both alternatives is acceptable for moderate seismic shaking, for very strong seismic shaking exceeding the design, the performance of the rocking-isolated system is advantageous: it survives with no damage to the columns, sustaining non-negligible but repairable damage to its beams and non-structural elements (infill walls, etc.). Copyright © 2011 John Wiley & Sons, Ltd.

Received 28 January 2011; Revised 30 September 2011; Accepted 3 October 2011

KEY WORDS: frame structure; capacity design; nonlinear dynamic analysis; foundation uplifting

1. INTRODUCTION

Earthquake engineering research has recognized that inelastic material response is inevitable under high levels of seismic attack, and that the increase of strength does not always result in enhanced safety. Hence, modern seismic design principles aim to control seismic damage rather than avoid it—*ductility* and *capacity* design. Global ductility levels of the order of three or more are allowed to develop, implying that the strength of a number of structural elements will be fully mobilized. With proper reinforcement detailing, it is intended to ensure that critical structural members can sustain deformations exceeding their capacity without collapsing, whereas failure 'is guided' to less important structural members (beams instead of columns) and to non-brittle mechanisms (bending instead of shearing) [1]. Yet, a growing population of researchers is currently pointing out the need of a skeptical look against the philosophy of current codes of practice. Performance-based design (i.e., design based on acceptable deformations, in general) has gained ground among structural engineers in contrast to the holistic applicability of the prevailing capacity design [e.g., 2–4], and has led to substantial improvements in modern seismic codes and regulations.

*Correspondence to: George Gazetas, Civil Engineering, National Technical University of Athens, Athens, Greece.
†E-mail: gazetas@ath.forthnet.gr

On the other hand, a crucial goal of current seismic *foundation* design, particularly as entrenched in the respective codes [e.g., 5], is to *avoid full mobilization of strength* in the foundation by '*guiding*' failure to the above-ground structure. The designer must ensure that the (difficult to inspect) below-ground support system will not even reach a number of 'thresholds' that would *statically* imply failure: mobilization of the soil-bearing capacity, significant foundation uplifting, sliding, or any combination are prohibited or severely limited. To this end, following the norms of capacity design, over-strength factors and (explicit or implicit) factors of safety are introduced against those 'failure' modes.

If such code provisions were relaxed, shallow foundations subjected to severe seismic shaking could experience either detachment from the supporting soil (because of large overturning moments and base shear) or deformation because of soil yielding. Yet, such a response does not necessarily imply failure—owing to the *cyclic* and *kinematic* nature of the seismic excitation. The mobilization of the above mechanisms may produce only limited deformations (rotation or displacement) prior to the reversal of the direction of motion, whereas the acceleration at the superstructure is bounded because of soil failure.

Performance-based design in earthquake geotechnics (i.e., design on the basis of limiting the displacements and rotations of facilities during the design earthquake) is a product of the previously mentioned consequences of the cyclic and kinematic nature of seismic motion. Thus, the concept of allowing significant *foundation uplifting* (geometric nonlinearity) and *mobilization of bearing capacity* mechanism (material inelasticity) during strong seismic shaking has been suggested in recent years as a deviation from the conventional design philosophy [6]. In fact, a significant body of pragmatic evidence provides justification of the idea that allowing nonlinear–inelastic foundation response may even be beneficial [7–19].

The time is therefore ripe for soil–foundation–structure interaction (SFSI) practice to also move from imposing 'safe' limits on forces and moments acting on the foundation, to performance–based design in which all possible pseudo-static 'failure' mechanisms are allowed to develop, provided that damage is maintained within acceptable limits. Such a new seismic design approach, in which soil failure acts as a safety 'fuse' for the superstructure (i.e., plastic 'hinging' is moved from the superstructure to the foundation soil) has been proposed by [9–11, 18, 20] among others. Using a simple bridge pier as an example, it was shown that this alternative may provide substantially larger safety margins (i.e., avoidance of collapse) for seismic motions that exceed the design limits, at the cost of increased foundation settlement.

This paper investigates the potential effectiveness of the aforementioned mechanisms (within the rationale of performance-based design) for the foundation of *frames*. Because foundation plastic 'hinging' is mainly intended to be in the form of foundation rocking and uplifting, the proposed design concept is termed *rocking isolation*. The idea of isolation through rocking is not a novelty to structural engineers. Motivated by the devastating Northridge (1994) earthquake, engineers devoted a significant amount of research on the development and promotion of novel isolating concepts. In these new typologies, the inelastic demand is accommodated within the connection itself (beam–column, column–foundation, wall–foundation critical interface) where a 'controlled rocking' motion occurs with opening and closing of the existing gap; as a consequence, a very limited level of damage is expected in structural members, which are maintained in the elastic range [21]. Such ideas have been explored among others by [22–27] who have manifested their beneficial effect on structures.

However, in the framework of the idea proposed herein, rocking isolation refers to foundation rather than structural members. Contrary to conventional capacity design, in the rocking isolation approach, footings are *under-designed* so that their moment capacity (M_{ult}) is lower than the bending moment capacity of the corresponding column. Hence, in case the earthquake demand exceeds the footing capacity, the latter is intended to uplift thus limiting the distress transmitted to the column (which responds elastically). Seismic waves propagate through the soil until its surface where the frame footings lie. Hence, the footings are subjected to an imposed acceleration at their base and, as a result, the amount of acceleration that will be transmitted to the superstructure is bounded by the yield acceleration of the footing (in the form of soil yielding or uplifting). Given that the superstructure follows the capacity design principles, plastic hinging on the ground floor (if any) will take place on the beam and not on the column. To illuminate the potential effectiveness of the *rocking isolation* concept to frame structures, an idealized simple but realistic two-story building is used as an illustrative example.

DOI: 10.1002/eqe

2. PROBLEM STATEMENT AND DESIGN CONSIDERATIONS

The problem analyzed is depicted in Figure 1. It refers to a fairly simple structure founded on a stiff clay layer (of undrained shear strength $S_u = 150$ kPa). Figure 1(a) and (b) compare schematically the differences between conventional *capacity* and *rocking isolation* design. In the first case, the design dictates that the footings are large enough to ensure sufficient fixity of the columns at their base. Their ultimate moment capacity is larger than that of the columns. Hence, the structure will respond to seismic loading through flexural distortion. Whenever the earthquake demand exceeds the capacity of the column M^C_{ult}, a plastic hinge develops at its base. Figure 1(c) illustrates the moment–curvature response of the RC column, designed according to EC8. The curvature ductility is defined as [28]:

$$\mu_\varphi = c_u / c_y \tag{1}$$

where c_y is the yield curvature of the reinforced concrete (RC) section (corresponding to initiation of plastic hinging) and c_u its ultimate curvature (corresponding to initiation of failure).

In the case of rocking isolation, the design of the superstructure follows exactly the same principles, but the capacity design for the foundation is reversed: the footings are *under-designed* to a lower moment capacity than that of the corresponding column. Therefore, whenever the earthquake demand tends to exceed the foundation capacity, the latter 'yields' through a combination of uplifting and mobilization of the bearing capacity failure mechanism. Indicative results for the moment–rotation response of the footing (for combined axial and shear force at a constant lever

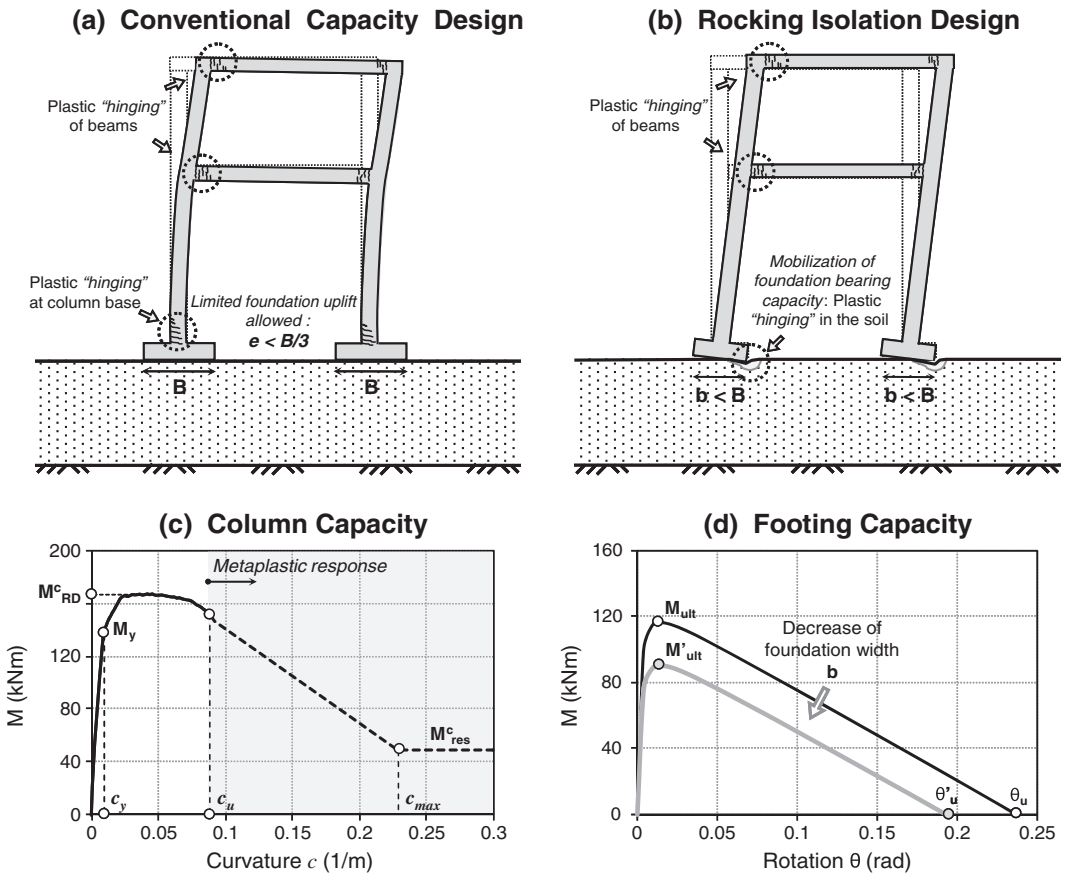

Figure 1. Comparison of (a) conventionally designed frame with (b) 'rocking-isolation' designed frame. (c) moment–curvature response of a RC column (ductile design, according to EC8 capacity design), and (d) moment–rotation response of the under-designed square footing, illustrating the effect of b reduction.

DOI: 10.1002/eqe

arm) resting on an over-consolidated clay layer (of $S_u = 150$ kPa, and $G_o = 200$ MPa) are depicted in Figure 1(d), demonstrating the effect of the reduced foundation width b. In accord with theoretical expectations, the decrease of the footing that leads to reduced moment capacity M_u and toppling rotation θ_u.

Geometry and member properties of the structure are shown in Figure 2. It consists of a one-bay two-story RC frame with a span of 5 m, ground floor height of 4 m, and first floor height of 3 m. The dimensions of structural members of the frame are summarized in Table I. The structure is designed in accordance to EC8 [5] and the Greek Reinforced Concrete Code [29], for a design acceleration $A_d = 0.36$ g, and behavior factor $q = 3.5$. The adopted dead and live loads ($G = 1.3$ kN/m^2 and $Q = 2$ kN/m^2) are typical values for residential buildings. The structure was analyzed and designed using conventional structural analysis software. Table I summarizes the computed internal forces of all structural members of the frame. The resulting reinforcement (applying capacity design), along with the bending moment strength M_{RD} of the structural members, are outlined in Table II.

2.1. *Conventional foundation design*

Obeying the capacity design principles (according to current Seismic Codes), the design overturning moment onto the foundation is calculated as

$$M_{Fd} = M_S + \psi M_E \tag{2}$$

where M_{FD} is the foundation moment capacity; M_S and M_E the moment because of *non-seismic* ($G + 0.3Q$) and *seismic* (E) loads (of the seismic load combination), respectively; and ψ an *over-strength* factor. The same calculations are performed for the design shear and axial forces on the footings (Table III).

According to most seismic codes (e.g., EC-7, DIN 4017) *and* the current state of practice, values of the eccentricity e (owing to the combined action of M and N) greater than one third of the footing width (*B/3)* dramatically reduce the bearing capacity of the footing. Taking account of code provisions and

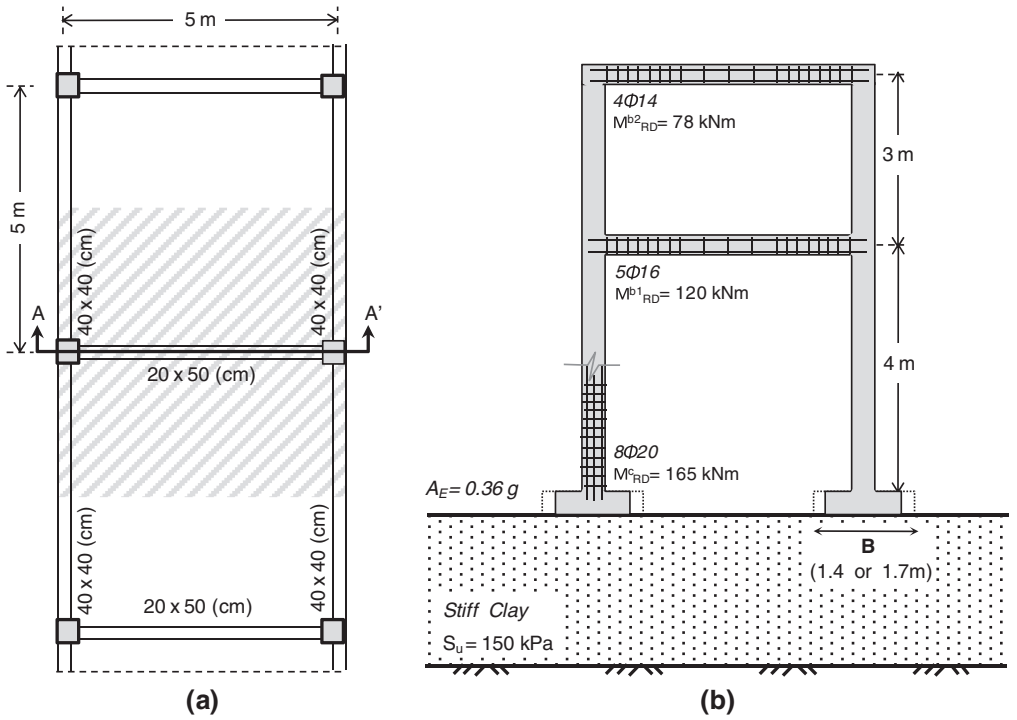

Figure 2. Geometry and member properties of the typical frame structure analyzed: (a) plan view, and (b) cross section A-A′.

DOI: 10.1002/eqe

Table I. Structural member dimensions of the idealized typical frame, and synopsis of computed internal forces for static and seismic load combinations.

Structural member	Dimensions (cm)	Static combination			Seismic combination					
		1.35 g + 1.5q			Vertical loading: g + 0.3q			Earthquake loading: ± E		
		M_S: kN m	Q_S: kN	N_S: kN	M: kN m	Q: kN	N: kN	M_E: kN m	Q_E: kN	N_E: kN
Ground floor columns–base	40 40	13	10	243	8	6	150	101	41	54
First floor columns–base	40 × 40	68	51	153	40	30	96	26	25	19
Ground floor beam–edges	20 × 50	71	117	0	41	68	0	80	35	0
First floor beam–edges	20 × 50	61	117	0	35	68	0	45	19	0

requiring safety factors for static and seismic loading of $FS_V \geqslant 3$ and $FS_E \geqslant 1$, respectively, the width of the square footing is conventionally computed as $B = 1.7$ m. With the eccentricity limitation being the controlling factor, the resulting safety factors for static and seismic loading turn out to be quite large: $FS_V = 8$ and $FS_E = 1.93$, respectively.

2.2. *Rocking-isolation foundation design*

Relaxing the eccentricity criterion, the footing is intentionally *under-designed* to a lower moment capacity than that of the column. Non-linear foundation response will depend on the achieved FS_V. To promote foundation uplifting rather than sinking because of excessive soil yielding, FS_V is required to be at least 3 [14, 15, 17–19, 30, 31]. Based on this requirement, Table IV summarizes the acceptable footing widths, along with their corresponding moment capacities M_{ult} (calculated according to [32]), the safety factors FS_V and FS_E, and the *capacity reduction factor (CRF)*, which is defined as

$$CRF = M_{RD}/M_{\text{ult}} \tag{3}$$

where M_{RD} is the column moment strength and refers to the *under-strength* factor of the foundation relative to the column. Large *CRF* values imply reduced foundation capacity, and hence, more intense rocking (hopefully resulting in more drastic cutoff of inertia forces transmitted onto the superstructure). On the other hand, as *CRF* tends to 1.0, the efficacy of rocking isolation is expected to be diminished.

Note that the applicability of the rocking isolation concept depends on the nature of the system. Although it may be effective for relatively slender systems, the response of which is dominated by the earthquake-induced bending moment (such as the one analyzed herein), it may not be an option for squatty structures (e.g., one-story frames), in which case the response is shear force-dominated;

Table II. Seismic capacity design of the superstructure: target moment capacity (M_{target}) of structural members, resulting longitudinal reinforcement, and achieved moment capacity (M_{RD}).

Structural member	Location	M_{target}: (kN m)	Reinforcement	M_{RD}: (kN m)
Ground floor columns	Top	119	8Ø20	165
	Bottom	146	8Ø20	165
First floor columns	Top	104	8Ø20	165
	Bottom	105	8Ø20	165
Ground floor beam	Edges	119	5Ø16	120
	Middle	64	3Ø14	67
First floor beam	Edges	79	4Ø14	80
	Middle	74	4Ø14	80

DOI: 10.1002/eqe

Table III. Forces acting on the footing for static and seismic load combinations.

	Static combination	Seismic combination		
	1.35 G + 1.5 Q	G + 0.3 Q	± E	EAK 2000*
M: kN m	13	8	100	186
Q: kN	10	6	41	78
N: kN	322	151	54	247

the absence of substantial moment M acting on the footing renders the $e \leqslant B/3$ criterion unimportant. On the other hand, multi-story frames are likely to demonstrate the effectiveness of this approach.

3. ANALYSIS METHODOLOGY

A characteristic 'slice' of the soil – structure system is analyzed employing the finite element (FE) method, taking account of material (soil and superstructure) and geometric (uplifting and P-Δ effects) nonlinearities (Figure 2(a)). As shown in Figure 3, whereas the soil and footings are modeled with appropriate nonlinear quadrilateral plane strain continuum elements, nonlinear beam elements are utilized for superstructure members.

Special interface elements at the soil-foundation interface allow both detachment and sliding. The latter obeys Coulomb's friction law, with detachment and uplifting arising from the tensionless interface behavior. 'Free-field' boundaries are utilized at the two lateral boundaries of the model. Nonlinear dynamic time history analysis is performed, applying the seismic excitation (i.e., acceleration time history) at the base of the model. The left and right side nodes of the model (on the same height) are connected by means of kinematic horizontal constraints. It is reasonable to assume that even elementary lateral boundaries, (placed at a distance of $10B$ from each footing, will be sufficient for the problem under study because only a negligible amount of radiation damping is generated, thanks to:

a. The dominant *rocking* mode, because of 'destructive interference' of the out-of-phase emitted waves from the two half-sides of the footing [34].
b. The fact that the fundamental shear–wave period, T_{soil} , of the soil layer is significantly lower than both the dominant period (T_E) of the earthquake and the natural period (T_{str}) of the superstructure [34]—especially in view of the fact that the latter increases substantially with uplifting.
c. The mobilization of the soil yielding and the formation of failure (sliding) surfaces create a soft zone under the footing, which reflects the incident waves [33,35].

3.1. Soil modeling

Nonlinear soil behavior is modeled through a simple kinematic hardening model with Von Mises failure criterion and associated flow rule. The full description of the model requires the knowledge of only three parameters: the elastic Young's modulus E, the strength σ_y , and the yield stress σ_o .

The model can be considered appropriate for clay under undrained conditions. Although phenomena such as pore-pressure buildup and dissipation cannot be captured, for the key aspects of the problem analyzed herein, undrained behavior may be considered a reasonable simplification provided that the stress σ_y of the Von Mises failure is related to the undrained shear strength S_u of the soil. Published G–γ curves [37, 38] were utilized to calibrate model parameters E and σ_o. The G/S_u ratio was assumed equal to 1000—a reasonable assumption for over-consolidated clay. The model has been successfully utilized [36] to reproduce foundation rocking experiments conducted at UC Davis [16, 17] and ELSA laboratory [15]. The former have been performed on clayey material with $FS_v = 5$, whereas the latter are 1-g tests on sand with $FS_v = 8$. Figure 4 compares the numerical prediction with experimental results. The model captures effectively the performance of the foundation, both in terms

DOI: 10.1002/eqe

Table IV. Alternative footing configurations: footing width B, resulting safety factor for static loading FS_V, moment capacity M_{ult} (computed analytically according to [32], assuming constant vertical load $N = 150$kN), and corresponding *Capacity Reduction Factor* (ratio of column capacity M_{RD} to the *f*ooting capacity M_{ult}). Footing widths below 1.1 m are not suggested, because the accomplished FS_V falls below 3.

Footing width B (m)	FS_V	M_{ult} for N = 150 kN (G + 0.3 Q)	Capacity reduction factor (CRF)
1.6	7.0	125	1.32
1.5	6.1	113	1.46
1.4	5.3	101	1.63
1.3	4.5	91	1.81
1.2	3.8	81	2.04
1.1	3.2	71	2.32

of moment–rotation (M–θ) and settlement–rotation (w–θ) response, under-predicting the hysteretic damping in clay. This under-prediction is considered acceptable, as it constitutes a conservative estimate of the effect of rocking isolation.

3.2. *Superstructure modeling*

For each structural member, the moment–curvature relationship up to the point of ultimate curvature c_u (Figure 1(c)) is first computed through static section analysis employing the XTRACT 2000 software (Imbsen & Associates, California, USA) [39]. The curvature ductility of the concrete sections modeled was of the order of $\mu_\varphi \approx 10$, reflecting well-reinforced sections according to EC8. Reasonable assumptions have been adopted for the metaplastic response of the section (i.e., $c > c_u$). The residual bending moment (M^c_{res}) of each RC section is assumed equal to 30% of the bending moment capacity [40], and is considered to be attained for a curvature three times larger (c_{max}) than the ultimate curvature c_u. The same kinematic hardening model is utilized, as suggested by Vesic [41], to simulate the nonlinear moment–curvature response of the superstructure RC members. Model parameters are calibrated against the target moment–curvature relationships computed by XTRACT. For a rectangular RC member of width d_b and height d_h, the strength σ_y can be defined as follows:

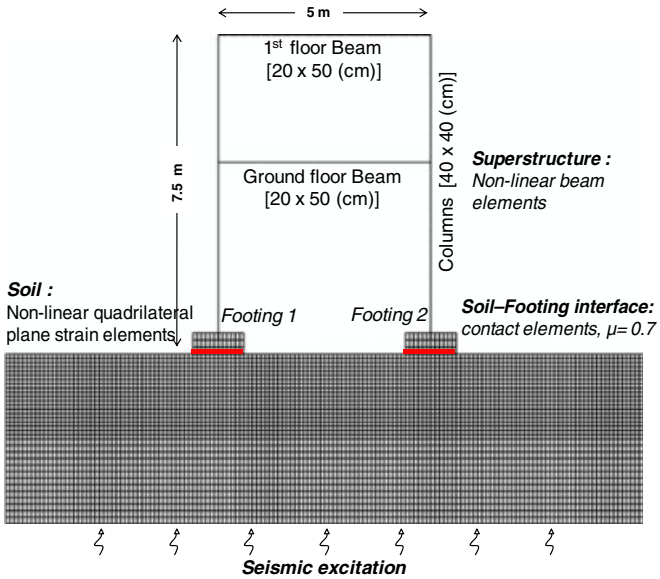

Figure 3. Finite element discretization: the system is modeled with due consideration to material (soil and superstructure) and geometric (uplifting and P–Δ effects) nonlinearities.

DOI: 10.1002/eqe

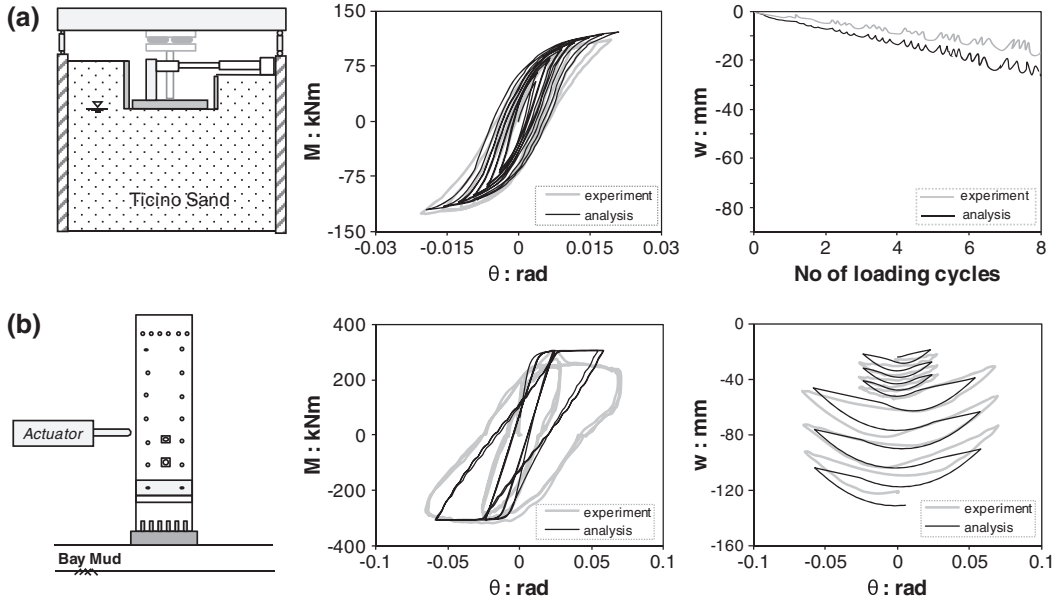

Figure 4. Validation of soil constitutive model. Comparison of predicted moment–rotation (M–θ) and settlement–rotation (w–θ) response with (a) experimental 1-g test results in sand [15], and (b) centrifuge model test results in clay [17].

$$\sigma_y = \frac{4M_y}{d_b d_h^2} \tag{4}$$

The small strain modulus C is equal to the Young's modulus of RC, whereas σ_o is estimated as $\sigma_y/10$. A user subroutine is encoded in ABAQUS (Dassault Systèmes Simulia Corp., Providence, RI, USA) [42] to reproduce the metaplastic softening response of RC sections, as well as stiffness degradation with deformation and cycles of loading.

The design with modern seismic codes implies sufficient hoop reinforcement to prevent cyclic strength degradation [40]. Therefore, such effect has been neglected in RC modeling. For similar reasons it has been considered adequate to neglect the possibility of reinforcement slippage (which may not be captured by the simplified model utilized herein) and assume perfect bond between concrete and steel bars. Figure 5(a) portrays the results of model calibration against monotonic static pushover loading of RC sections. The FE simulation of the response of the sections under cyclic loading of gradually increasing displacement amplitude is shown in Figure 5(b) and (c). Figure 5(b) displays the moment–curvature loops (up to the point of ultimate curvature c_u) taking account of stiffness degradation, whereas the loops produced when neglecting stiffness degradation are portrayed in Figure 5(c). This behavior has been deliberately neglected in the subsequent analyses (although neglecting stiffness degradation in fact promotes the conventional design scheme over the proposed rocking-isolation) to eliminate the dependence of the behavior of either of the two design alternatives on material behavior. However, it should be noted that several hysteretic models have been developed to accurately model RC hysteretic response that can be used in future studies.

3.2.1. Equivalence of 2D with 3D analysis. The analysis is conducted under quasi two-dimensional (2D) conditions, considering a representative *equivalent* 'slice' of the soil-structure system. To render the 2D foundation model 'equivalent' to the square 3D problem, the Meyerhof [43] and Vesic [44] bearing capacity shape factor of 1.2 (for square foundation) was applied to the out-of-plane dimension of the soil 'slice' of the model. This procedure does not reproduce the elastic stiffness of the foundation as accurately.

DOI: 10.1002/eqe

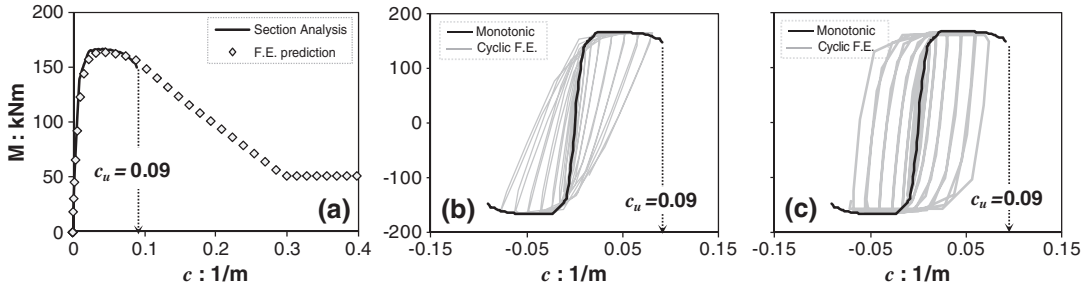

Figure 5. Superstructure modeling. (a) calibration against monotonic moment–curvature (M–c) response calculated through conventional RC section analysis up to the ultimate curvature c_u , and applying reasonable assumptions for the metaplastic part of the response (i.e., for $c > c_u$); FE computed M–c response for cyclic loading up to the point of ultimate curvature c_u: (b) taking account of stiffness degradation, and (c) ignoring stiffness degradation [results shown for 40×40 cm column, with $8\Phi20$ longitudinal reinforcement].

To verify the validity of such equivalence, two FE models (Figure 6(a)) were developed to simulate the response of a one-DOF system to cyclic lateral loading: a rigorous 3D model, and an 'equivalent' 2D model (Figure 6(a)). The footing has a width $B = 1.7$ m and bears a vertical load $N = 150$ kN. Figure 6(b) and (c) compares the results of the two models in terms of moment–rotation and settlement–rotation response of the footing, for two idealized soil profiles: a homogeneous hard clay of undrained shear strength $S_u = 150$ kPa (typical of over-consolidated clay) and a moderately soft clay of $S_u = 50$ kPa. In accord with experimental and theoretical evidence [16, 17, 19, 30, 45], for the case of clays, when the static safety factor FS_V is relatively large, (e.g., $FS_V > 3$, as with the stiff clay of $S_u = 150$ kPa), the response of the footing is dominated by uplifting (Figure 6(b)); for relatively small safety factors, for example, $FS_V < 2$ (as with the $S_u = 50$ kPa), the response is dominated by accumulating settlement (Figure 6(c)). In the former case (stiff soil), the equivalent 2D model reproduces, with reasonable accuracy, the results of the 3D FE model. In the latter case, the equivalent 2D model slightly under-predicts (by less than 10%) the cyclic settlement, whereas

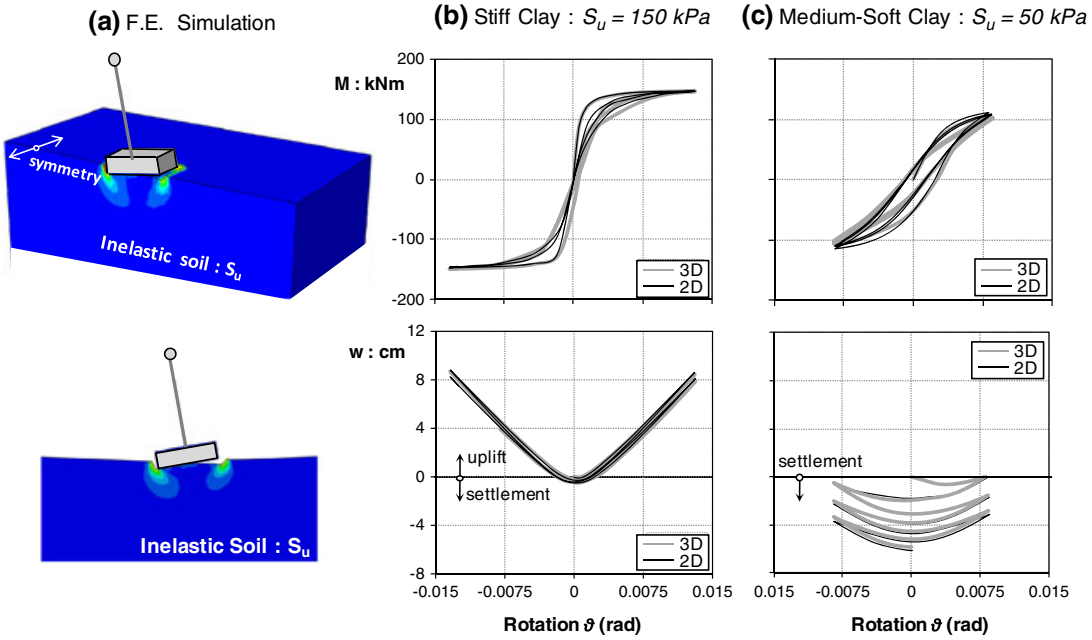

Figure 6. Comparison of rigorous 3D with 'equivalent-2D' FE analysis results in terms of (a) deformed mesh with superimposed plastic strain contours; moment–rotation (M–θ) and settlement–rotation (w–θ) response of $B = 1.7$-m square footing founded on: (b) $S_u = 150$ kPa clay, and (c) $S_u = 50$ kPa medium-soft clay.

DOI: 10.1002/eqe

the ultimate moment M_{ult} is barely over-predicted (by less than 5%). The overall hysteretic damping and the footing rotation are captured quite effectively. Overall, the equivalent 2D approach reproduces the key aspects of the 3D problem very effectively, and is hence adopted for the subsequent parametric analyses.

4. STATIC PUSHOVER ANALYSIS: INSIGHT ON THE ROCKING BEHAVIOR OF FRAMES

4.1. System response

The rocking response of frames differs substantially from that of one-DOF systems, such as the one discussed in the previous section. To gain insight on the mechanisms controlling its response, the model frame is first subjected to static displacement-controlled lateral pushover loading, taking account of P–Δ effects. Figure 7 compares the response of the conventional system ($B = 1.7$-m footings), with

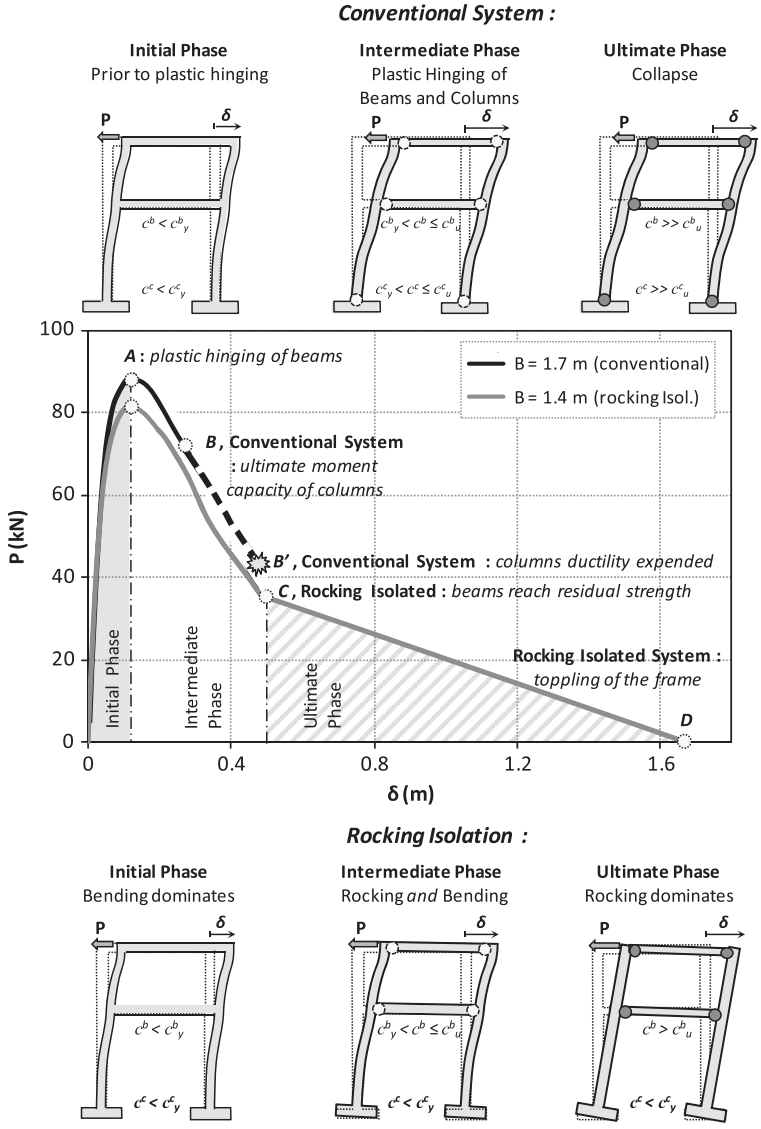

Figure 7. Static pushover P–Δ curves of the two design alternatives: the conventional system with large (over-designed) $B = 1.7$-m footings compared with the 'rocking-isolated' system with smaller (under-designed) $B = 1.4$-m footings (corresponding to a capacity reduction factor of 1.6).

DOI: 10.1002/eqe

the rocking-isolated alternative ($B = 1.4$-m footings). System response can be divided into three characteristic phases: (i) an *initial phase*, in which column bending dominates and the two alternatives exhibit nearly identical behavior; (ii) an *intermediate phase*, in which both column bending and foundation rocking take place—the former dominating in the conventional design (until its capacity is fully mobilized) and the latter in the new design; and (iii) the *ultimate phase*, which for the rocking-isolated alternative is dominated by foundation rocking; the conventional system collapses.

In the *initial phase*, the two frames respond to the imposed lateral loading mainly through flexural deformation (bending), with the conventional developing slightly larger resisting force P. The reaction force is maximized on the onset of beams yielding (point A in the diagram). This behavior clearly respects the weak beam—strong column capacity design.

In the *intermediate phase*, the columns of the conventionally designed system are pushed beyond their yield curvature c_y until they eventually reach their ultimate theoretical curvature c_u (i.e., when their ductility capacity is completely expended: point B′ in the diagram). After this point, collapse is imminent. In contrast, the rocking-isolated frame responds to increasing δ with footing detachment, uplifting and substantial rotation: the under-designed foundations reach their (limited) moment capacity first, thereby limiting the distress transmitted to the columns. Hence, the response of the latter remains within the elastic range throughout this phase. Still, the beams keep accumulating plastic deformation until their residual strength (point C)—the end of the intermediate phase. The residual strength of the beams is assumed to be constant—a simplification that is unavoidable at this stage of analysis, but not necessarily realistically safe.

In the *ultimate* phase, the conventional system has collapsed, while the rocking isolated system reduces from its initial state (frame structure) to two approximately one-DOF systems connected to each other through the two-hinged beams. During this phase, further increase of the imposed displacement δ leads to further accumulation of footing rotations until the structure ultimately topples and the reaction force P reaches zero under the action of gravity only because of P–Δ effects.

4.2. *Foundation response*

Figure 8 compares the M–θ response of the left and right $B = 1.4$-m footings under static pushover analysis. The left footing develops significantly lower moment, not exceeding 80 kN m compared with over 120 kN m for the right one, but its toppling rotation is larger ($\theta_{ult} = 0.25$ rad, as opposed to 0.18 rad for the right footing). These quite pronounced differences are attributed to the complex mechanisms governing the behavior of the multi-DOF frame. Naturally, as the column spacing to height ratio increases, axial load fluctuations diminish, and the difference between the two columns becomes less pronounced. The redistribution of internal forces among the frame structural members and the subsequent progressive failure of beams result in fluctuation of both the axial force N, and the moment to shear force ratio M/Q transmitted on to each footing during loading. As explained in the sequel, the combination of N and M/Q greatly affects the rocking response of the two footings.

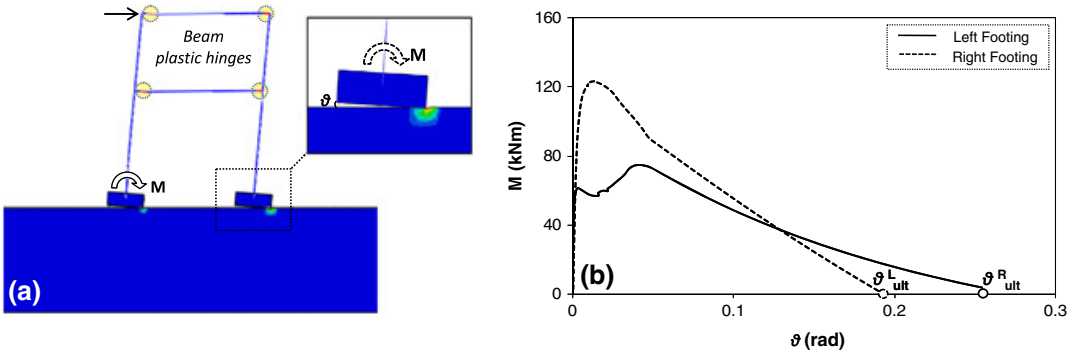

Figure 8. Static pushover analysis: (a) deformed mesh with superimposed plastic shear strain contours; and (b) moment-rotation (M–θ) response of the two footings.

DOI: 10.1002/eqe

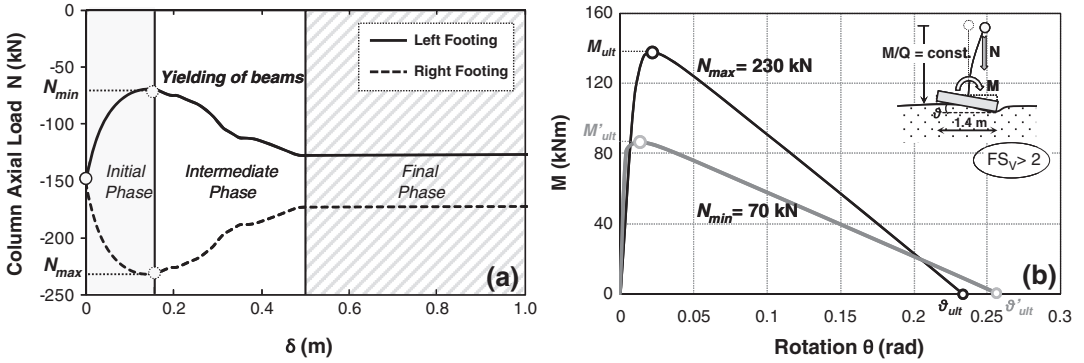

Figure 9. Static pushover analysis: (a) evolution of the axial load N of the two columns as a function of the imposed lateral displacement δ; and (b) schematic illustration of the effect of N on the moment capacity of the footing ignoring the frame action. (Results shown for the $B = 1.4$ m alternative, considering the extreme forces $N_{\min}$ and $N_{\max}$ as constantly applied).

4.2.1. The effect of axial load fluctuation on footing response. Figure 9(a) displays the evolution of the axial load N of the two columns with imposed displacement δ, with due reference to the three previously identified phases of system response. During the *initial phase*, increasing δ leads to an increase of N on the right column ($N_{\max} = 230$ kN) and an equal decrease on the left ($N_{\min} = 70$ kN), as their sum remains constant, equal to the total vertical load of the superstructure. This reflects the frame reaction to lateral loading, with development of a pair of axial forces on the columns, in addition to bending moments M and shear forces Q. In the subsequent *intermediate phase*, during plastic hinging of the beams, the *frame action* gradually diminishes and both columns tend to 'retreat' towards their initial static value of 150 kN. In fact, the assumption of a non-zero and constant residual moment capacity of beams is the only reason why N is not becoming exactly equal to its original value (a small bending moment is still transmitted, and a limited *frame action* remains). The axial column load is constant throughout the *ultimate phase*. This observation is consistent with the previous analogy with a hybrid system of two idealized one-DOF oscillators.

Figure 9(b) illustrates the effect of N on the M–θ (moment–rotation) response of the $B = 1.4$-m footing, ignoring the frame action (i.e., considering an equivalent one-DOF system of constant height). As expected [32, 46–48], provided that the static safety factor FS_V of the footing is substantially larger than two, M_{ult} increases with increasing N.

This justifies the augmented value of the maximum moment achieved in the right footing, as well as the rapid drop of the moment on the left footing during the initial phase depicted on Figure 7. In the context of rocking-isolation design, an increase of M_{ult} is not desirable as it amplifies the risk of increasing the amount of bending moment that may be transmitted by the footing onto the column, hence jeopardizing the structural integrity of the latter. Therefore, such effects must be carefully investigated.

4.2.2. Effect of M/Q fluctuation on foundation response. Figure 10(a) displays the evolution of the M/Q ratio versus the imposed lateral displacement δ, with reference again to the three phases of system response. In the initial phase, as the frame is still 'undamaged' (no plastic hinging has yet developed), M/Q varies between about 2 and 2.5 m—quite a similar result to that of a conventional pseudostatic analysis of the frame assuming full fixity conditions on its base (Table I, seismic load combination, ground floor columns: $M/Q = 2.46$ m).

During the *intermediate phase*, as the beams gradually reach their residual moment capacity, M/Q is asymptotically approaching the height of the center of mass of the system (4.82 m), but without actually reaching it. This is endorsed to the fact that the column–beam connection never actually reduces to an ideal hinge because the residual strength of the beam does not vanish.

In the *ultimate phase*, the M/Q ratio diminishes again. The footing has reached its moment capacity M_{ult}, and the corresponding column bending moment cannot possibly further enlarge. But this is hardly the case with the shear force: because the lateral horizontal capacity of the footing has not yet been reached, the column base shear may increase further to undertake the additional imposed lateral

DOI: 10.1002/eqe

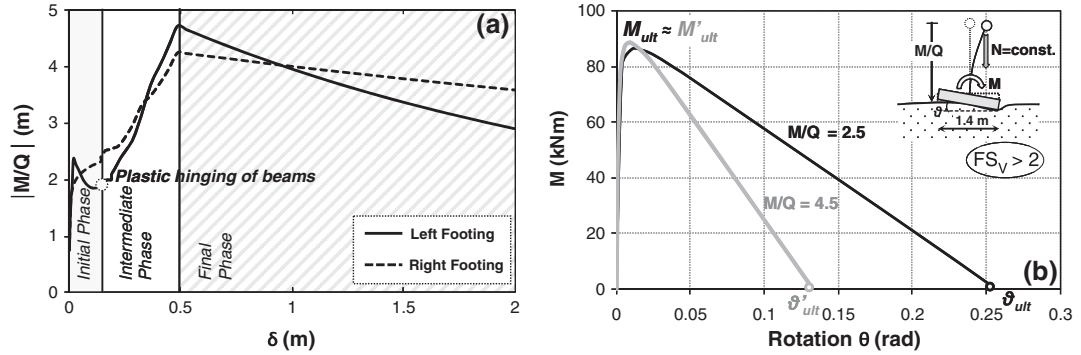

Figure 10. Static pushover analysis: (a) evolution of *M/Q* with imposed lateral displacement δ. During the *initial phase*, no plastic hinging has developed and *M/Q* fluctuates between 1.8 and 2.4 m. During the *intermediate phase*, as plastic hinging develops, and frame action tends to diminish, *M/Q* increases to 4.5 m. In the *final phase*, *M/Q* decreases slightly; (b) illustration of the effect of *M/Q* on the moment–rotation response of the footing of a one-DOF system (results shown for the $B = 1.4$ m alternative, for constant $N = 150$ kN).

loading. Therefore, because the moment acting on the footing remains constant (M_{ult}) whereas the shear force keeps increasing, the *M/Q* ratio unavoidably recedes.

The effect of the *M/Q* ratio is of particular significance for rocking-isolation design: it affects the rotation capacity θ_{ult} of the footing and consequently the overall ductility of the system. To further elucidate this effect, Figure 10(b) illustrates the effect of *M/Q* on the *M–θ* (moment–rotation) response of the $B = 1.4$-m footing ignoring the frame action (i.e., considering an equivalent one-DOF system of constant $N = 150$ kN equal to the initial static value). Obviously, θ_{ult} (and hence, rotational ductility) decreases substantially with increasing *M/Q*: for low values of *M/Q* (i.e., for $M/Q = 2.5$ m corresponding to the *initial phase*, when the frame is still undamaged) $\theta_{ult} \approx 0.25$, whereas for $M/Q = 4.5$ m (corresponding to the ultimate phase with plastic hinges developed in the beams) $\theta_{ult} \approx 0.13$ (almost 50% decrease). On the other hand, at least for the quite high M/Q ratio ranges examined, the capacity of the footing is quite insensitive to *M/Q*.

5. DYNAMIC ANALYSIS: COMPARISON OF CONVENTIONAL WITH ROCKING-ISOLATED SYSTEM

The seismic performance of the two design alternatives (conventional, $B = 1.7$ m; rocking-isolated, $B = 1.4$ m) is further elucidated through a series of nonlinear dynamic time history analyses in which the FE model is subjected to a wide range of seismic motions: 24 earthquake records of worldwide historic events. Given in Figure 11 along with their acceleration (*SA*) and velocity (*SV*) elastic response spectra, the selected records can broadly be categorized into moderately strong (close to design acceleration levels), and very strong seismic motions. They cover a wide range of strong-motion parameters such as *PGA*, *PGV*, *SA*, *SV*, frequency range, number of strong-motion cycles, and duration; near source (directivity and fling-step) effects are embodied in many of these records.

5.1. Fundamental period of the frame

The fundamental period of the fully fixed superstructure, considering elastic behavior is calculated as $T_{sup} = 0.38$ s. This value is considerably increased because of the effect of soil-structure interaction. For the case of elastic soil, the fundamental period of the system, taking account of the previously mentioned effects, may be approximately calculated as:

$$T = T_{\sup}\sqrt{1 + \frac{K}{K_{xx}} + \frac{KH}{K_r} + \frac{KH^2}{K_t}} \tag{5}$$

where H is the initial *M/Q* ratio acting at the foundation level, and K_{xx}, K_r, and K_t the horizontal, rocking, and torsional stiffness of the foundation, respectively [49]. With this, the fundamental (i.e., initial, elastic)

DOI: 10.1002/eqe

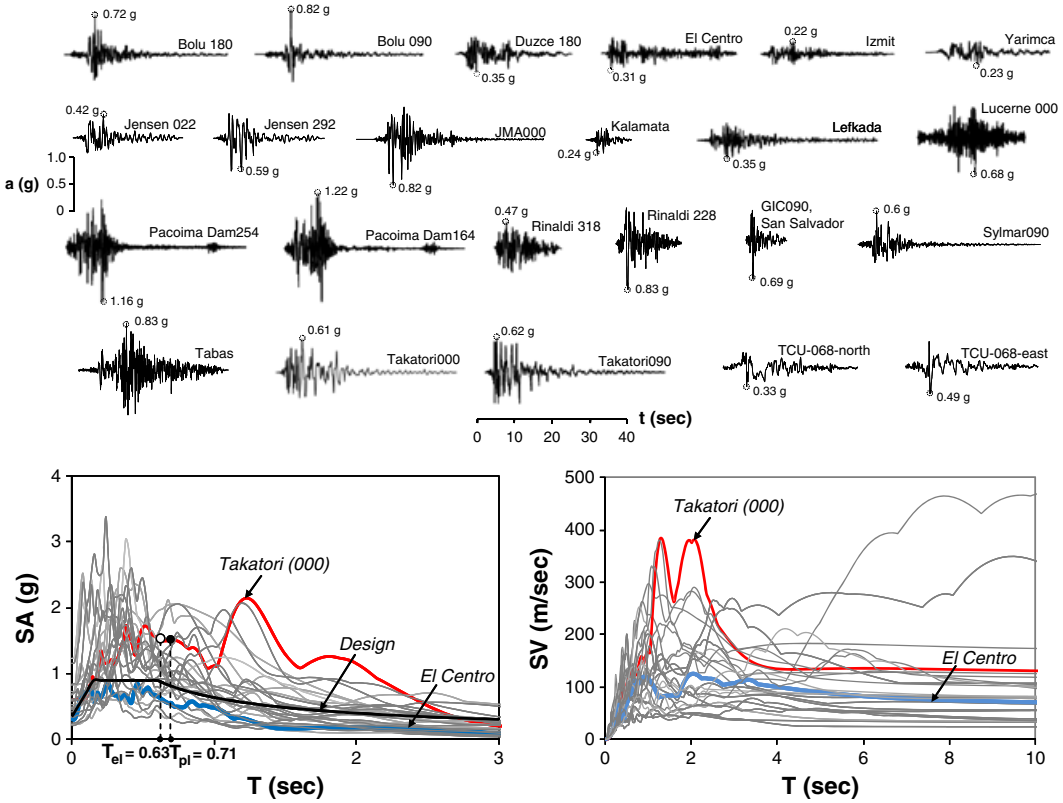

Figure 11. The 24 original earthquake records utilized as excitation for the analysis of the two alternatives, along with their acceleration and velocity response spectra. Covering a range from medium to very strong seismic events, they collectively encompass the effects of forward-rupture directivity, multiple cycles, fling-step.

period of the soil-structure system is calculated as $T_{\rm el} = 0.63$ s for $B = 1.7$ m, and $T_{el} = 0.70$ s for the $B = 1.4$-m footings. These values are in full accord with the results of FE analysis, considering elastic soil response. When soil non-linearity is taken into account, these values rise to $T_{pl} = 0.71$ and 0.75 s for the $B = 1.7$ and 1.4-m footings, respectively (calculated during the very early phase of monotonic loading when the response may be considered as quasi-elastic).

The fundamental (i.e., initial) periods of the two alternatives are also marked on Figure 11. Apparently, the behavior of the structures examined herein may, by no means, be considered as reflective of a favorable effect of 'classic soil structure interaction (SSI)'. On the contrary, especially in case of large period records (e.g., Takatori) the present study further corroborates earlier findings by [50], showing that SSI may even be detrimental. Thus, the present study will be focusing on highlighting the beneficial effect of the concept of rocking isolation on the seismic behavior of frame structures. SSI effects are either way incorporated in the results, as they can be fully captured by the coupled numerical model.

The seismic performance of the two alternatives is first compared in detail for two characteristic cases: (a) moderately strong seismic shaking, utilizing the El Centro 1940 record as seismic excitation, which is close to, but always less severe than the elastic design spectrum; and (b) very strong seismic shaking, utilizing the Takatori (Kobe 1995) record, which substantially exceeds the design spectrum of the frame. In the first case, the objective is to explore the performance of the two alternatives, mainly in terms of *serviceability* after a design level seismic shaking. In the latter case, the focus is on *safety* in case of an 'unanticipated' event that substantially exceeds the design. Results for the complete set of motions are then shown in summary for each alternative.

5.2. *Performance in moderately strong seismic shaking*

The two design alternatives are subjected to the El Centro record of the M_s 7.2 Imperial Valley 1940 earthquake [51]. As illustrated in Figure 11, this seismic motion may be considered roughly equivalent to

DOI: 10.1002/eqe

the 'design earthquake'. The comparison of the two alternatives is portrayed in Figure 12 in terms of (a) column bending moment–curvature (M–c) response (revealing the 'consumption' of superstructure ductility); (b) foundation moment–rotation (M–θ) response (revealing the 'consumption' of foundation ductility); (c) foundation settlement–rotation (w–θ) response; and (d) time history of ground floor drift δ. The latter consists of two components: (i) the 'flexural drift' δ_c (i.e., the lateral displacement of the structure because of flexural distortion of its structural members), and (ii) the 'rocking drift' $\delta_R = \theta h$ (i.e., the lateral displacement at height h owing to foundation rocking of angle θ). The flexural drift δ_c is a direct indicator of damage inflicted on RC frame elements (i.e., columns and beams). On the other hand, the overall differential (top-to-base) displacement of the structure (and, hence, the damage of non-structural members) is more directly related to the total drift δ.

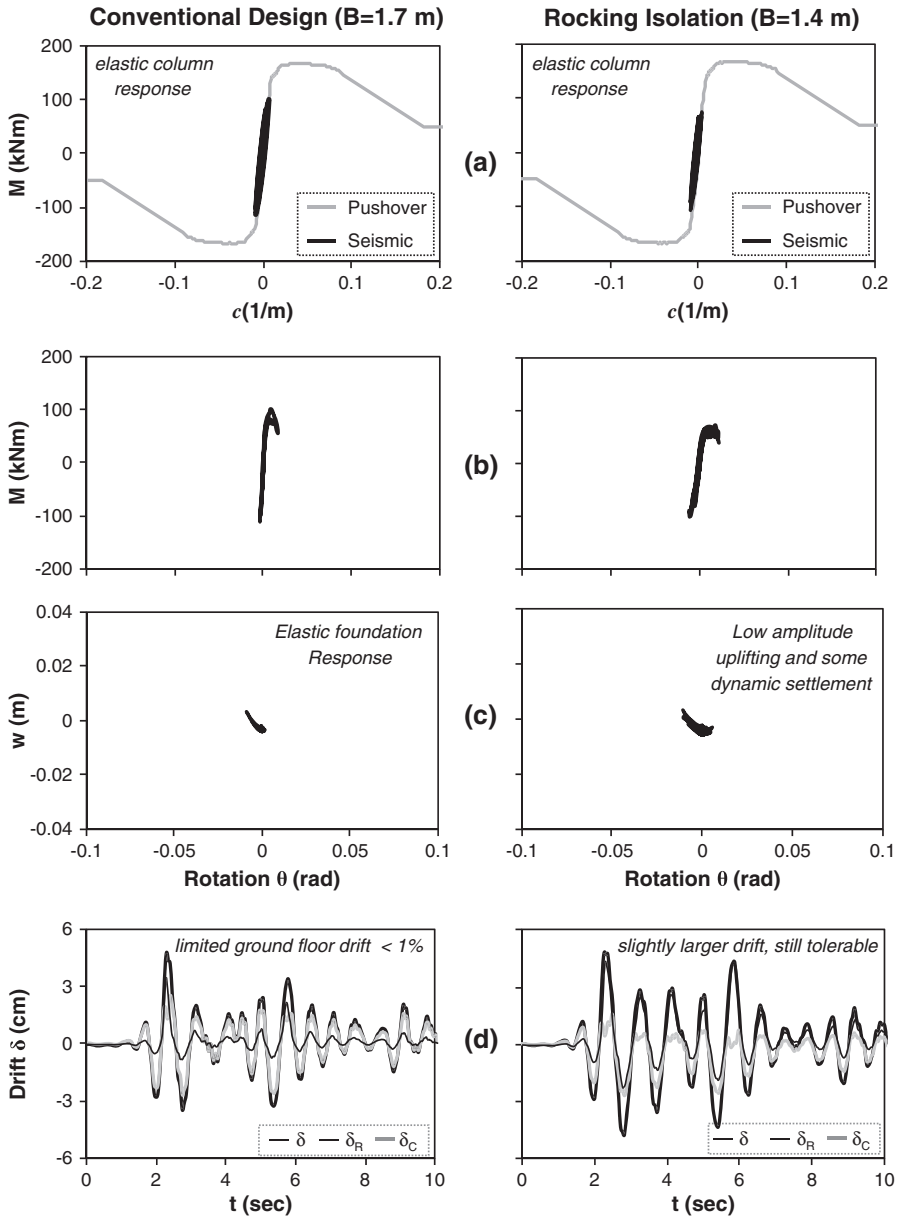

Figure 12. Performance of the two design alternatives (conventional, $B = 1.7$ m; rocking isolation, $B = 1.4$ m) subjected to moderately strong seismic shaking (El Centro record), in terms of: (a) column bending moment–curvature (M–c) response; (b) foundation overturning moment–rotation (M–θ) response; (c) foundation settlement–rotation (w–θ) response; and (d) time history of ground floor drift δ.

DOI: 10.1002/eqe

As revealed by the column M–c response (Figure 12(a)), both structures react almost elastically. Also (essentially) elastic is the response of the foundations of both alternatives (Figure 12(b)). The $B = 1.4$-m footings of the rocking-isolated alternative experience slightly more intense uplifting than those of the conventional system, but the rotation θ is maintained within essentially the same (very low) levels. The same applies to the shaking-induced settlement w, which in both cases remains well within serviceability limits (Figure 12(c)).

Nevertheless, the unconventionally designed footing responds mostly by uplifting, contrary to the bending-dominated behavior of the conventional frame. This can be appreciated in Figure 12(d): although the maximum total drift δ is practically the same for the two alternatives, a significant discrepancy may be observed in the contribution of the two drift-generating mechanisms (i.e., *flexural distortion* and *rocking*). In the conventional system, the response is dominated by flexural distortion, with δ being predominantly related to δ_c; in the rocking-isolated alternative δ_R contributes much more than δ_c in the development of the total drift δ.

5.3. *Performance in very strong seismic shaking*

The Takatori record of the M_s 7.2 Kobe 1995 earthquake is utilized to explore the performance of the two alternatives when shaken well beyond the limits of the design. As shown in Figure 11, with a *PGA* of 0.70 g, *PGV* of 169 cm/s, and encompassing the effect of forward rupture directivity and soil amplification, this record is considered one of the worst seismic motions ever recorded. In terms of *SA*, it exceeds the design by a factor of at least two over the whole period range. As depicted in Figure 13(a), the conventionally designed system cannot withstand this level of ground shaking. Plastic hinges first develop at the beams, and later in the two columns. The ensuing severe accumulation of plastic curvature expends the available column ductility (Figure 13(b)), and the frame is unavoidably led to collapse.

In stark contrast, the rocking-isolated alternative succeeds in surviving the tremendous seismic shaking, with its columns behaving almost elastically: because the moment capacity of the footing is lower than the bending moment capacity of the column, the latter is protected from structural damage by foundation yielding (mainly through uplifting and very limited mobilization of soil failure). Naturally, in terms of foundation M–θ response the picture is reversed (Figure 13(c)). In the conventional system, the large $B = 1.7$-m footings never reach their ultimate capacity; once the columns have failed (i.e., their ductility capacity has been reached), θ increases 'infinitely' because of the collapse of the structure. On the contrary, in the case of the rocking-isolated alternative, the smaller $B = 1.4$-m footings reach their moment capacity several times during seismic shaking, as a result of intense uplifting and rocking. Yet, this behavior is not accompanied by augmented permanent settlement; despite the fact that the seismic settlement w is indeed larger for the rocking-isolated alternative, this increase should not be of concern because its absolute value does not exceed a mere 1 cm. As evidenced by Figure 13(d), whereas the large footings of the conventional alternative are subjected to limited rocking oscillation and uplifting, the smaller footings of the rocking-isolated structure are subjected to noticeable uplifting and develop larger rotations. However, the residual rotation at the end of shaking is insignificant: a direct result of the inherent self-centering behavior of rocking foundations. Owing to this behavior, the rotation developed during seismic shaking (and the subsequent footing uplifting) may be fully recovered after the earthquake because of the action of gravity, provided that the factor of safety against vertical loads is adequately high, so as to ensure uplifting dominated response.

This behavior is further reflected in the time history of inter-story drift portrayed in Figure 13(e). During shaking, the total drift δ reaches 40 cm indicating serious distortion of the superstructure. Yet, this distortion is mainly due to foundation rotation (rocking-induced drift δ_R), being only slightly associated with column structural damage (flexural drift δ_C). Consequently, the residual δ of the ground floor is limited to no more than 5 cm, corresponding to a drift ratio $\delta/h \approx 2\%$ (where h is the height of the story). Conversely, for the conventionally designed system, column failure is caused by pure flexural drift (black and gray lines on the plot coincide). In conclusion, the structural integrity of frame columns (which is associated with δ_C) is not jeopardized despite the severity of

DOI: 10.1002/eqe

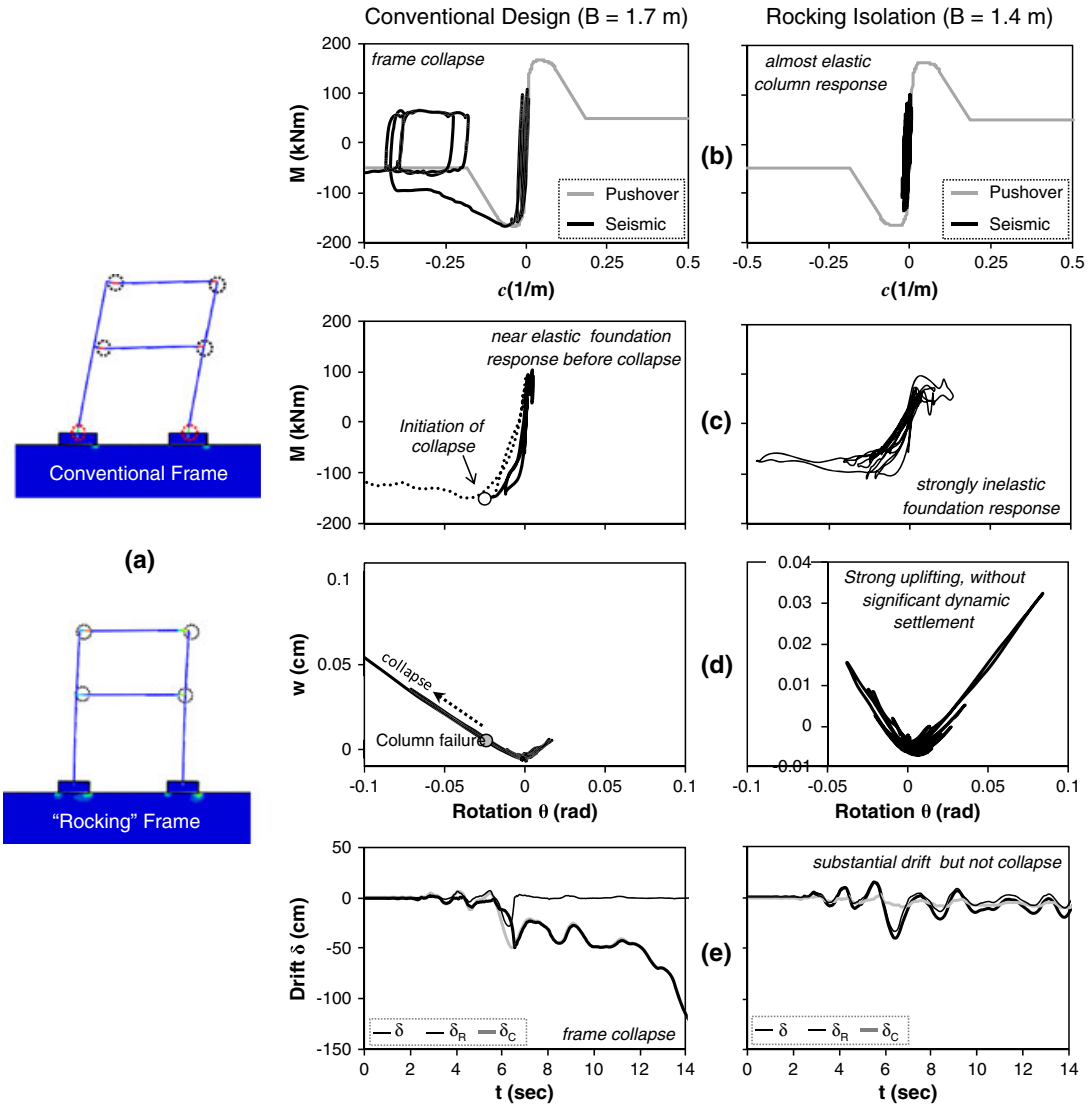

Figure 13. Performance of the two design alternatives (conventional, $B = 1.7$ m; rocking isolation, $B = 1.4$ m) subjected to very strong seismic shaking (Takatori record). (a) deformed system with plastic shear deformations; (b) column bending moment–curvature (M–c) response; (c) foundation overturning moment–rotation (M–θ) response; (d) foundation settlement–rotation (w–θ) response; and (e) time history of ground floor drift δ.

the earthquake scenario (in which the conventionally designed system would collapse), but damage to beams (which consume all their ductility capacity) and to non-structural elements (such as infill walls, etc.) cannot be avoided.

6. SYNOPSIS AND CONCLUSIONS

The performance of the two design alternatives is summarized in Figure 14 for all investigated earthquake scenarios (24 seismic excitations). Key performance indicators are plotted against the peak spectral pseudo-velocity, maximum *PSV*, of the seismic excitation (undoubtedly far more representative than *PGA* or *PSA* for inelastic systems). Following [28], three limit states may be defined regarding the performance of the frame, related to the flexural drift ratio (δ_c/h):

DOI: 10.1002/eqe

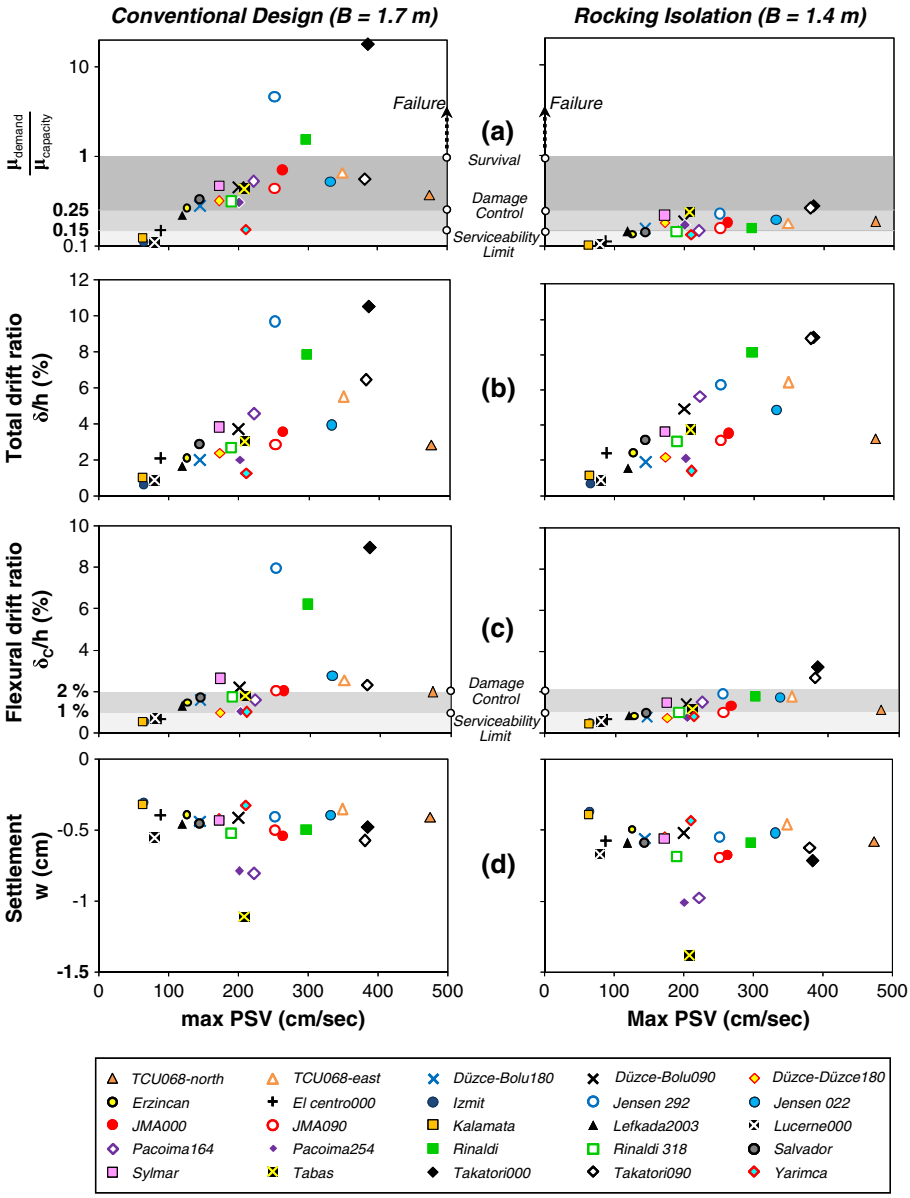

Figure 14. Summary of the response of the two design alternatives as a function of the maximum spectral velocity *SV*: (a) column curvature ductility demand over capacity ratio; damage level is indicated with reference to *response limit states* [21]; (b) total drift ratio for the ground floor δ/h (where h is the height of the ground floor); (c) flexural drift ratio δ_C/h; and (d) settlement w of the footing center.

a. The *serviceability limit state*, for $\delta_c/h \leqslant 1\%$, in which the structure can be fully functional after the earthquake, without the need for significant remedial measures;
b. The *damage control limit state*, for $1\% < \delta_c/h \leqslant 2\%$, in which the structure is expected to sustain repairable damage, but the cost of repair should be substantially lower than the cost of replacement;
c. The *survival limit state*, for larger δ_c/h, in which the collapse of the structure may be marginally avoided, although structural damage will be excessive and replacement will be unavoidable.

Figure 14(a) and (b) outlines the performance of the two systems in terms of ground floor column 'ductility consumption' ratio $\mu_{\text{demand}}/\mu_{\text{capacity}}$ and the flexural drift ratio δ_c/h. As previously discussed, the available ductility of the RC column is $c_u/c_y \approx 10$ (see also Figure 1(b)). Naturally,

DOI: 10.1002/eqe

for moderately strong seismic motions close to *the design limits* (e.g., El Centro) the performance of the conventional system is excellent; when damage does occur, it is controllable. However, for records exceeding the design (e.g., JMA, Tabas), damage is substantial and most times irreparable. For extreme seismic shaking (such as Takatori-000, and Jensen-292), μ_{demand} may be an order of magnitude larger than μ_{capacity}, and frame collapse is almost inevitable. Note that by no means should such performance be interpreted as a shortcoming of conventional capacity design. In fact, this is totally consistent with the whole philosophy of current seismic design, according to which the superstructure is designed to sustain extensive plastic hinging, possibly leading to irreparable damage, but avoiding collapse and serious foundation damage.

On the other hand, it is evident that the performance of the rocking-isolated alternative is definitely superior, with column damage being within the *serviceability limit state* for almost 50% of the seismic excitations investigated herein, and within *damage control* for the rest. For all 24 seismic excitations examined, the vast majority of which exceeds the design, the column damage is maintained within repairable limits. In other words, this study confirms previous research findings (e.g., [19, 30] indicating that damping associated with foundation rocking can be very significant at high rotational angles (e.g.,,>2%).

Figures 14(b) and (c) compare the performance of the two design alternatives in terms of total δ/h and flexural δ_c/h ground floor drift ratios. In all cases, the two design schemes display similar behavior in terms of total δ/h, with the rocking-isolated system performing marginally better and with less scatter about a mean line. The picture is of course conspicuously different in terms of flexural drift δ_c/h, which for the rocking isolated case is insignificant whereas it contributes almost exclusively towards the total drift in the conventional case. However, because the total drift ratio δ/h is practically the same, damage of beams and of non-structural elements is practically similar for the two structures. In terms of settlement (Figure 14(d)), the performance of the two design alternatives is quite similar, with the rocking-isolated system performing marginally worse. This differs substantially from what was concluded for one-DOF systems [20], in which case the rocking-isolated system was found to sustain substantially increased settlement. This key difference is attributable to the relatively large static safety factor ($FS_V = 5.3$ for $B = 1.4$ m) of the system examined herein, which promotes uplifting rather than 'sinking' behavior of the footing.

In conclusion, the concept of rocking isolation has been proposed as an effective means of reducing the earthquake demand on low rise frames. Further investigation is required to extend its applicability to high-rise frame structures. The main outcomes of the study are:

- *For moderately strong seismic excitations within the design limits*, the performance of both design alternatives is practically equivalent: they would both survive the earthquake, sustaining acceptable structural damage. With conventional design, structural damage would be repairable (flexural cracking of beams and columns), but not necessarily within the serviceability limits. In contrast, the rocking-isolated structure would suffer rather minor structural damage (flexural cracking of beams), and could most probably be utilizable immediately after the earthquake.
- *For very strong seismic shaking, well in excess of the design limits*, the performance of the rocking-isolated system may be quite advantageous. The conventionally designed frame may collapse (in roughly 13% of the seismic scenarios examined) or sustain non-repairable damage (to its beams *and* columns). By contrast, the rocking-isolated frame would survive, sustaining repairable but non-negligible damage to its beams and non-structural elements (infill walls, etc.). In any case, for such extreme seismic shaking, for which avoidance of collapse is the main objective, the rocking-isolation approach seems to lead to a robust design. For the studied cases in particular, in which the static bearing capacity safety factor of even the under-designed footings is quite large ($SF^s > 5$), seismic settlements are hardly a serious issue. It is noted, however, that results refer to simplified example and could be further validated for more complex structures.

In view of these , it is envisaged that the concept of rocking isolation may be considered as a valid seismic design alternative for new structures (especially in the case of unusually large frames, in which code limitations may hardly be met), but (perhaps) even more importantly for retrofitting existing structures: strengthening of the superstructure (to achieve compatibility with current seismic codes), but abolishing the need to strengthen the foundation, as well (a rather daunting task, indeed).

DOI: 10.1002/eqe

ACKNOWLEDGEMENT

This work forms part of the EU research project 'DARE' ('Soil–Foundation–Structure Systems Beyond Conventional Seismic Failure Thresholds: Application to New or Existing Structures and Monuments'), which is funded by the European Research Council 'Ideas' Programme: Support for Frontier Research—Advanced Grant, under contract number ERC-2008-AdG 228254-DARE.

REFERENCES

1. Paulay T. A simple displacement compatibility-based design strategy for reinforced concrete buildings. Proceedings of the 12th World Conf. on Earthquake Eng. 2000; Paper No.0062.
2. Bertero VV. Strength and deformation capacities of buildings under extreme environments. *Structural Engineering and Structural Mechanics* 1980; Vol. Honoring EP, Popov K (eds). Prentice-Hall: Englewood Cliffs NJ; 188–237.
3. Tassios TP. Seismic design: state of practice. Proceedings of 11th European Conference on Earthquake Engineering 1998; Rotterdam, AA Balkema: 255–267.
4. Priestley MJN. Performance-based seismic design. Proc. 12th World Conference on Earthquake Engineering, Auckland, New Zealand 2000; Paper No. 2831.
5. EC8, Design provisions for earthquake resistance of structures, part 5: foundations, retaining structures and geotechnical aspects. prEN, 1998–5 European Com. for Standardization, Brussels, 2000.
6. FEMA 356, *Prestandard and Commentary for the Seismic Rehabilitation of Buildings*. Federal Emergency Management Agency: Washington DC, 2000.
7. Huckelbridge AA. Jr., Clough RW. Seismic response of uplifting building frame. *Journal of the Structural Division* 1978; **104**(8):1211–1229.
8. Psycharis I. Dynamics of flexible systems with partial lift-off. *Earthquake Engineering and Structural Dynamics* 1983; **2**:201–521.
9. Yim CS, Chopra AK. Earthquake response of structures with partial uplift on Winkler foundation. *Earthquake Engineering and Structural Dynamics* 1984; **12**:263–281.
10. Nakaki DK, Hart GC. Uplifting response of structures subjected to earthquake motions. Report No. 2.1-3, U.S.–Japan Coordinated Program for Masonry Building Research 1987.
11. Pecker A. Capacity design principles for shallow foundations in seismic areas. Proc. 11th European Conference on Earthquake Engineering, AA. Balkema Publishing, 1998.
12. Pecker A. A seismic foundation design process, lessons learned from two major projects: the Vasco de Gama and the Rion Antirion bridges. *ACI Int. Conf. on Seismic Bridge Design and Retrofit*, La Jolla, ACI: Michigan, USA, 2003.
13. Martin GR, Lam IP. Earthquake resistant design of foundations: retrofit of existing foundations. *Proc. GeoEng Conference*, GeoEng 2000: Melbourne, AU (VIC), 2000.
14. Pecker A, Pender MJ. Earthquake resistant design of foundations: new construction. Invited paper. *GeoEng Conference, Melbourne* 2000, **1**:313–332.
15. Faccioli E, Paolucci R, Vivero G. Investigation of seismic soil–footing interaction by large scale cyclic tests and analytical models. Proc. 4th International Conference on Recent Advances in Geotechnical Earthquake Engrng and Soil Dynamics 2001; Paper no. SPL-5, San Diego, California.
16. Kutter BL, Martin G., Hutchinson TC, Harden C., Gajan S., Phalen JD. *Status report on study of modeling of nonlinear cyclic load-deformation behavior of shallow foundations*. Univ. of California, Davis, PEER Workshop: California, USA, 2003.
17. Gajan S, Kutter BL, Phalen JD, Hutchinson TC, Martin GR. Centrifuge modeling of load-deformation behavior of rocking shallow foundations. *Soil Dynamics and Earthquake Engineering* 2005; **25**:773–783
18. Kawashima K, Nagai T, Sakellaraki D. Rocking seismic isolation of bridges supported by spread foundations. *Proc. of 2nd Japan-Greece Workshop on Seismic Design, Observation, and Retrofit of Foundations, Tokyo, Japan* 2007; **1**:254–265.
19. Paolucci R, Shirato M, Yilmaz MT. Seismic behaviour of shallow foundations: shaking table experiments versus numerical modelling. *Earthq. Engnrng and Struct. Dynamics* 2008; **37**:577–595.
20. Anastasopoulos I, Gazetas G, Loli M, Apostolou M, Gerolymos N. Soil failure can be used for earthquake protection of structures. *Bulletin of Earthquake Engineering* 2010; **8**:309–326.
21. Priestley MJN, Seible F, Calvi GM. *Seismic Design and Retrofit of Bridges*. John Wiley & Sons: N.Y, 1996.
22. Stanton JF, Stone WC, Cheok GS. A hybrid reinforced precast frame for seismic regions. *PCI Journal* 1997; **42**(2):20–32.
23. Christopoulos C, Filiatrault A, Folz B. Seismic response of self-centering hysteresis SD and F systems. *Earthquake Engineering and Structural Dynamics* 2002; **31**:1131–1150.
24. Mander JB, Chen CT. Seismic resistance of bridge piers based on damage avoidance design. Technical Report NCEER-97-0014, SUNY, Buffalo, 1997.
25. Priestley MJN, Sritharan S, Conley JR, Pampanin S. Preliminary results and conclusions from the PRESSS five-story precast concrete test-building. *PCI Journal* 1999; **44**(6):42–67.
26. Hewes JT, Priestley MJN. "Seismic Design and Performance of Precast Concrete Segmental Bridge Columns." *Structural Systems Research Project, Report No. SSRP– 2001/25*, University of California: San Diego, La Jolla, California, 2002.
27. Kawashima K. Seismic design of concrete bridges. *Proc., 1st FIB Congress*, JCI, Japan Concrete Institute: Osaka, 2002; 347–366

DOI: 10.1002/eqe

28. Priestley MJN, Calvi GM, Kowalsky MJ. *Displacement-Based Seismic Design of Structures*. IUSS Press: Pavia, Italy, 2007, ISBN: 88-6198-000-6.
29. EKOS, *Greek code for reinforced concrete*. Org. of Seismic Planning and Protection: Athens, 2000.
30. Gajan S, Kutter B. Capacity, settlement, and energy dissipation of shallow footings subjected to rocking. *Journal of Geotechnical and Geoenvironmental Engineering ASCE* 2008; **134**(8):1129–1141.
31. Chatzigogos CT, Pecker A, Salencon J. Macroelement modeling of shallow foundations. *Soil Dynamics and Earthquake Engineering* 2009; **29**(6):765–781.
32. Gourvenec S. Shape effects on the capacity of rectangular footings under general loading. *Geotechnique* 2007; **57**(8): 637–646.
33. Poulos HG, Davis EH. *Elastic Solutions for Soil and Rock Mechanics*, Wiley: NY 1974.
34. Kausel E. Forced vibrations of circular foundations on layered media. *M.I.T. Research Report R74-11, Soils Publication No. 336, Structures Publication No. 384*, MIT, Cambridge, 1974.
35. Borja RI, Wu WH, Amies AP, Smith HA. Nonlinear lateral, rocking, and torsional vibration of rigid foundations. *Journal of Geotechnical Engineering, ASCE* 1994; **120**(3):491–513.
36. Anastasopoulos I, Gelagoti F, Kourkoulis R, Gazetas G. Simplified constitutive model for simulation of cyclic response of shallow foundations: validation against laboratory tests. *Journal of Geotechnical and Geoenvironmetal Engineering, ASCE* 2010 DOI: 10.1061/(ASCE)GT.1943-5606.0000534.
37. Vucetic M, Dobry R. Effect of soil plasticity on cyclic response. *Journal of Geotechnical Engineering, ASCE* 1991; **117**(1):89–107.
38. Ishibashi I, Zhang X. Unified dynamic shear moduli and damping ratios of sand and clay. *Soils and Foundations* 1993; **33**(1):12–191.
39. Imbsen and Associates, Inc. *XTRACT—Cross Section Analysis Program for Structural Engineer*, Ver. 3.0.3, California, 2004.
40. Vintzileou E, Tassios TP, Chronopoulos M. Experimental validation of seismic code provisions for RC columns. *Engineering Structures* 2007; **29**:1153–1164.
41. Gerolymos N, Gazetas G, Tazoh T. Seismic response of yielding pile in non-linear soil. *Proc. 1st Greece–Japan Workshop on Seism. Design, Observation, and Retrofit of Fndns*., Athens, 2005: 25–36.
42. ABAQUS, Inc. ABAQUS user's manual, Providence, R.I. 2009.
43. Meyerhof GG. Some recent research on the bearing capacity of foundations. *Canadian Geotechnical Journal* 1963; **1**(1):6–26.
44. Vesic AS. Analysis of ultimate loads of shallow foundations. *Journal of Soil Mechanics Foundation Div., ASCE* 1973; **99**, No. SM1: 45–73.
45. Allotey N, El Naggar MH. Analytical moment–rotation curves for rigid foundations based on a Winkler model. *Soil Dynamics and Earthquake Engineering* 2003; **23**:367–381.
46. Houlsby GT, Puzrin AM. The bearing capacity of a strip footing on clay under combined loading. Proceedings of the Royal Society of London, 1999; 893–916.
47. Bransby MF. Failure envelopes and plastic potentials for eccentrically loaded surface footings on undrained soil. *Int. Journal for Numerical and Analytical Methods in Geomechanics* 2001; **25**:329–346.
48. Taiebat HA, Carter JP. Bearing capacity of strip and circular foundations on undrained clay subjected to eccentric loads. *Geotechnique* 2002; **52**(1):61–64.
49. Gazetas G. Analysis of machine foundation vibrations: state of the art. *Soil Dynamics and Earthq. Engineering* 1983; **2**:2–41.
50. Mylonakis G, Gazetas G. Seismic soil–structure interaction: beneficial or detrimental? *Journal of Earthquake Engineering* 2000; **4**(3):277–301.
51. Trifunac MD. Tectonic stress and the source mechanism of the Imperial Valley, California earthquake of 1940. *Bulletin of the Seismological Society of America* 1972; **62**(5):1283–1302.

DOI: 10.1002/eqe